JOURNAL OF MATHEMATICAL PHYSICS VOLUME 44, NUMBER 9 SEPTEMBER 2003

Symmetry and pattern formation for a planar layer of nematic liquid crystal

David Chillingworth[a)]
Department of Mathematics, University of Southampton, Southampton SO17 1BJ, United Kingdom

Martin Golubitsky[b)]
Department of Mathematics, University of Houston, Houston, Texas 77204-3476

(Received 6 February 2003; accepted 12 May 2003)

Using equivariant bifurcation theory, and on the basis of symmetry considerations independent of the model, we classify square and hexagonally periodic patterns that typically arise when a homeotropic or planar isotropic nematic state becomes unstable, perhaps as a consequence of an applied magnetic or electric field. We relate this to a Landau–de Gennes model for the free energy, and derive dispersion relations in sufficient generality to illustrate the role of up/down symmetry in determining which patterns can arise as a stable bifurcation branch from either initial state. © *2003 American Institute of Physics.* [DOI: 10.1063/1.1598620]

I. INTRODUCTION

There is an extensive amount of literature on spatially periodic pattern-formation in physical and biological systems: see for example the surveys by Cross and Hohenberg (1993) and Cladis and Palffy-Muhoray (1995). The mathematical techniques to analyze the creation and interactions of such patterns often involve reduction of the governing partial differential equations to a finite-dimensional system that captures the essential dynamics near a bifurcation point of a fundamental equilibrium state, followed by a bifurcation analysis to classify the branching of multiple solutions.

The crucial role of *symmetry* in organizing pattern-forming bifurcations has been recognized for some time: see Busse (1962); Buzano and Golubitsky (1983); Golubitsky *et al.* (1984), for example. Indeed, on the basis of symmetry considerations alone, and with some natural nondegeneracy assumptions, a classification of branching behavior for systems with symmetry can be given that is independent of the actual mathematical model. This insight, with the associated technical machinery of group theory and group actions, is the inspiration for the texts such as Golubitsky *et al.* (1988); Chossat and Lauterbach (2000); Golubitsky and Stewart (2002). The general theory provides a framework: in order to make specific predictions of physical behavior exerimental numerical values (or sometimes just their signs) need to be determined, unfortunately not necessarily an easy task.

In this paper we generalize methods that have been previously and successfully applied in other fields (Buzano and Golubitsky, 1983; Golubitsky *et al.*, 1984; Golubitsky *et al.*, 1988; Bressloff *et al.*, 2001a; Golubitsky and Stewart, 2002) to the context of pattern formation in planar liquid crystals. A preliminary version of our results appears in Golubitsky and Chillingworth (2003). We consider periodic planar patterns with square or hexagonal symmetry that can bifurcate from a homeotropic or planar isotropic state. We do not claim to predict experimental conditions under which these states can be observed; rather we set out a dictionary of possibilities on the basis of natural mathematical assumptions. Numerous patterns similar to those we describe have indeed been observed in liquid crystal experiments, see, e.g., de Gennes (1974); Huh *et al.* (2000), but under conditions often quite different from ours. The question of how to detect experimentally

[a)]Electronic mail: drjc@maths.soton.ac.uk
[b)]Electronic mail: mg@uh.edu

the variety of director-field patterns predicted here is one that we are not yet in a position to answer. However, we do give some pointers on dealing with this issue by calculating key aspects of branching behavior for an explicit Landau–de Gennes type model.

II. THE GENERAL STRATEGY

In the Landau theory of phase transitions for a liquid crystal the degree of coherence of alignment of molecules is usually represented by a *tensor order parameter*, a field of symmetric 3×3 tensors $Q(\mathbf{x})$, $\mathbf{x}\in\mathbf{R}^3$ with $\mathrm{tr}(Q)=0$ (Sluckin, 2000). We think of Q as the second moment of a probability distribution for the directional alignment of a rod-like molecule. In a spatially uniform system, Q is independent of $\mathbf{x}\in\mathbf{R}^3$. When $Q=0$ the system is *isotropic*, with molecules not aligned in any particular direction. If there is a preferred direction along which the molecules tend to lie (but with no positional constraints) the liquid crystal is in *nematic* phase. There are many other types of phase involving local and global structures, see Sluckin (2000).

In this paper we consider a thin planar layer of nematic liquid crystal where the top and bottom boundary conditions on this layer are identical. In this situation the symmetries of any liquid crystal model will include planar Euclidean symmetries $\mathbf{E}(2)$ as well as up/down reflection symmetry.

A configuration or *state* of a liquid crystal is often described by a director field (a unit length vector field) that assigns to each point $\mathbf{x}$ in the planar layer a unit vector $\mathbf{n}(\mathbf{x})$ in the direction in $\mathbf{R}^3$ along which molecules tend to align. In this description $\mathbf{n}(\mathbf{x})$ and $-\mathbf{n}(\mathbf{x})$ are not distinguished. We approximate a planar layer by a plane—so for us a liquid crystal state consists of a three-dimensional director field $\mathbf{n}$ defined on $\mathbf{R}^2$.

In the Landau theory the direction of $\mathbf{n}(\mathbf{x})$ is just an eigenvector corresponding to the largest eigenvalue of $Q(\mathbf{x})$—the direction in which a molecule has the ''maximum probability'' of aligning. We shall refer to $Q(\mathbf{x})$ also as the *state* of the system. If $Q(\mathbf{x})$ has two (or three) equal maximum eigenvalues then $\mathbf{n}(\mathbf{x})$ is undefined (a dislocation occurs), whereas the tensor field $Q(\mathbf{x})$ is everywhere defined, continuous and in our case analytic.

In our discussion we assume an initial equilibrium state Q_0 that is $\mathbf{E}(2)$-invariant. Because of translation symmetry such states are spatially uniform and because of rotation symmetry they have the form

$$Q_0=\eta\begin{bmatrix}-1 & 0 & 0\\ 0 & -1 & 0\\ 0 & 0 & 2\end{bmatrix}$$

for some nonzero $\eta\in\mathbf{R}$. For $\eta>0$ the state Q_0 represents a *homeotropic* phase (the state has constant alignment in the vertical direction), whereas for $\eta<0$ it represents a planar *isotropic* liquid crystal (a molecule is equally likely to align in any horizontal direction). The state Q_0 is also invariant under up/down reflection, that is conjugacy by the matrix

$$\tau=\begin{bmatrix}1 & 0 & 0\\ 0 & 1 & 0\\ 0 & 0 & -1\end{bmatrix}.$$

We consider models for equilibria that are determined internally by a free energy rather than externally by, say, a magnetic field. Thus, the symmetry group for our discussion is

$$\Gamma=\mathbf{E}(2)\times\mathbf{Z}_2(\tau),$$

since these are the symmetries of both the initial state Q_0 and the model.

Our aim in this paper is to study local bifurcation from Q_0 to states that have spatially varying alignment along the plane. Specifically, we consider bifurcation to states exhibiting spatial peri-

odicity with respect to some planar lattice. Following Golubitsky *et al.* (1988) and Golubitsky and Stewart (2002) we use group representation theory to extract information about nonlinear behavior near bifurcation that is independent of the model.

There is a common approach to all lattice bifurcation problems, which we now describe. This discussion, adapted from Bressloff *et al.* (2001a), will be familiar to anyone who has studied pattern formation in Bénard convection models, although there are minor differences due to the change in context. See Golubitsky *et al.* (1988); Golubitsky and Stewart (2002).

Let λ be a bifurcation parameter and assume that the equations have Q_0 as an equilibrium for all λ. Let L denote the equations linearized about Q_0. In the models, λ is the temperature and bifurcation occurs as λ is decreased.

(1) A linear analysis about Q_0 leads to a *dispersion curve*.

Translation symmetry in a given direction implies that (complex) eigenfunctions have a *plane wave factor* $w_{\mathbf{k}}(\mathbf{x})=e^{2\pi i\mathbf{k}\cdot\mathbf{x}}$ where $\mathbf{k}\in\mathbf{R}^2$. Rotation symmetry implies that the linearized equations have infinite-dimensional eigenspaces; instability occurs simultaneously to all functions $w_{\mathbf{k}}(\mathbf{x})$ with constant $k=|\mathbf{k}|$. The number k is called the *wave number*. Points (k,λ) on the dispersion curve are defined by the maximum values of λ for which an instability of the solution Q_0 to an eigenfunction with wave number k occurs.

(2) Often, the dispersion curve has a unique maximum, that is, there is a *critical* wave number k_* at which the first instability of the homogeneous solution occurs as λ is decreased.

Bifurcation analyses near such points are difficult since the kernel of the linearization is infinite-dimensional. This difficulty can be side-stepped by restricting solutions to the class of possible solutions that are doubly periodic with respect to a planar lattice $\mathcal{L}$.

(3) The symmetries of the bifurcation problem restricted to $\mathcal{L}$ change from Euclidean symmetry in two ways.

First, translations act on the restricted problem modulo $\mathcal{L}$; that is, translations act as a torus $\mathbf{T}^2$. Second, only a finite number of rotations and reflections remain as symmetries. Let the *holohedry* $H_{\mathcal{L}}$ be the group of rotations and reflections that preserve the lattice. The symmetry group $\Gamma_{\mathcal{L}}$ of the lattice problem is then generated by $H_{\mathcal{L}}$, $\mathbf{T}^2$, as well as (in our case) $\mathbf{Z}_2(\tau)$.

(4) The restricted bifurcation problem must be further specialized. First, a *lattice type* needs to be chosen (in this paper square or hexagonal). Second, the *size* of the lattice must be chosen so that a plane wave with critical wave number k_* is an eigenfunction in the space $\mathcal{F}_{\mathcal{L}}$ of matrix functions periodic with respect to $\mathcal{L}$.

Those $\mathbf{k}\in\mathbf{R}^2$ for which the scalar plane wave $e^{2\pi i\mathbf{k}\cdot\mathbf{x}}$ is $\mathcal{L}$-periodic are called *dual wave vectors*. The set of dual wave vectors is a lattice, called the *dual lattice*, and is denoted by $\mathcal{L}^*$. In this paper we consider only those lattice sizes where the critical dual wave vectors are vectors of shortest length in $\mathcal{L}^*$. Therefore, generically, we expect $\ker\mathsf{L}=\mathbf{R}^n$ where n is 4 and 6 on the square and hexagonal lattices, respectively.

(5) Since $\ker\mathsf{L}$ is finite-dimensional, we can use Liapunov–Schmidt or center manifold reduction to obtain a system of reduced bifurcation equations on $\mathbf{R}^n$ whose zeros are in 1:1 correspondence with the steady states of the original equation. Moreover, this reduction can be performed so that the reduced bifurcation equations are $\Gamma_{\mathcal{L}}$-equivariant.

(6) Solving the reduced bifurcation equations is still difficult. A partial solution can be found as follows. A subgroup $\Sigma\subset\Gamma_{\mathcal{L}}$ is *axial* if $\dim\mathrm{Fix}(\Sigma)=1$ where

$$\mathrm{Fix}(\Sigma)=\{x\in\ker\mathsf{L}:\sigma x=x \quad \forall\sigma\in\Sigma\}.$$

The Equivariant Branching Lemma (Golubitsky *et al.*, 1988) states that generically there exists a branch of solutions corresponding to each axial subgroup. These solution types are then classified by finding all axial subgroups, up to conjugacy.

On general grounds, when restricting attention to bifurcations corresponding to shortest wavelength vectors, we may assume the representation (action) of $\Gamma_{\mathcal{L}}$ to be irreducible: see Golubitsky *et al.* (1988); Chossat and Lauterbach (2000). In Sec. III we show that there are four distinct types of irreducible representation of $\Gamma_{\mathcal{L}}$ that can occur in bifurcations from Q_0. These representations

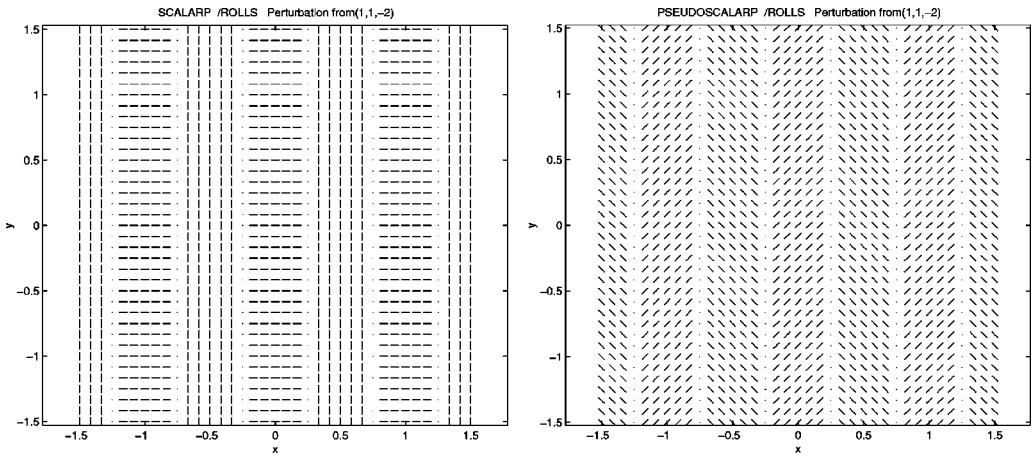

FIG. 1. Stripes from isotropic ($\eta<0$) state with $\tau=+1$ representations: scalar ''martensite'' (left); pseudoscalar ''chevron'' (right). Note that $\cdot$ in the figures indicates points where $Q(\mathbf{x})$ has a double maximum eigenvalue.

are the four combinations of (i) scalar or pseudoscalar (see Bosch Vivancos *et al.*, 1995; Bressloff *et al.*, 2001a; Golubitsky and Stewart, 2002) and (ii) preserve or break τ symmetry. In Sec. III we also compute the axial subgroups for each of these representations and draw pictures of each of the relevant planforms on the square and hexagonal lattices.

Note that line fields near hometropic are almost vertical, whereas line fields near isotropic are almost horizontal. In our figures, where we view the perturbed line fields from above, we see the planar projections of the line field in all cases. We also see the deviation from vertical and, through foreshortening of the line field elements, the deviation from horizontal. However, in this presentation, we cannot distinguish the ''up'' and ''down'' ends of the line field elements. It is an elementary yet curious observation that in Landau models restricted to a planar layer, bifurcations from the homeotropic phase ($\eta>0$) do not lead to clear new patterns unless τ symmetry is broken: the τ symmetry ''freezes'' the director field to the vertical. This point is discussed in more detail in Sec. III. Therefore we present pictures of the four bifurcations from the isotropic case ($\eta<0$) and only the two bifurcations when τ acts as -1 in the homeotropic case ($\eta>0$). The $\tau=+1$ bifurcations in the homeotropic case can lead to patterns in a theory posed on a thickened planar layer. In such a theory, which goes beyond what we present here, the precise form of boundary conditions on the upper and lower boundaries of the layer will determine the pattern types. In the other bifurcations, the contributions to pattern selection of these boundary conditions should be less important.

In fact, the bifurcation theory for each of these four representations of $\Gamma_{\mathcal{L}}$ has been discussed previously in different contexts. It is only the interpretation of eigenfunctions in the context of $Q(\mathbf{x})$ that needs to be computed, along with the pictures of the resulting planforms. More specifically, when τ acts trivially on $\ker \mathsf{L}$ the scalar representation has been used in the study of pattern formation in Rayleigh–Bénard convection by Busse (1962) and Buzano and Golubitsky (1983), and the pseudoscalar representation has been studied by Bosch-Vivancos, Chossat, and Melbourne (1995) and also in the context of geometric visual hallucinations by Bressloff *et al.* (2001b); (2001a). When τ acts nontrivially the two representations have the same matrix generators and although the planforms are different for these two representations the bifurcation theory is identical. Indeed, this theory is just the one studied for Rayleigh–Bénard convection with a midplane reflection by Golubitsky, Swift, and Knobloch (1984).

Perhaps the most interesting patterns that appear from our analysis are the stripes or ''rolls'' (from convection studies) type patterns that bifurcate from the isotropic state when τ symmetry is not broken, that is $\tau=+1$. The scalar pattern is a ''martensite'' pattern whereas the pseudoscalar pattern is a ''chevron'' pattern. See Fig. 1. The fact that such patterns do occur in liquid crystal layers is well known: see, for example, de Gennes (1974), and also Huh *et al.* (2000) from which

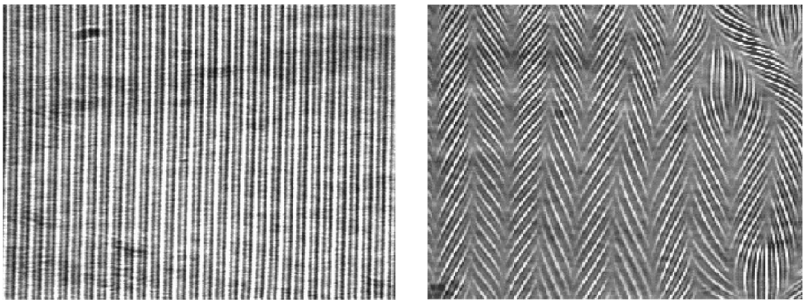

FIG. 2. Rolls (left) and chevrons (right). (Pictures courtesy of J.-H. Huh.)

the pictures in Fig. 2 are taken. However, it is important to emphasize that these patterns were observed under experimental conditions far removed from those to which our theoretical model applies. Moreover, the observed chevrons exhibit additional fine periodic structure (which renders them visible as chevrons and not stripes) that we do not discuss here. We recall that patterns described in this paper are those that can arise close to homeotropic or planar isotropic states.

In Sec. IV we introduce free energies that illustrate that all four representations can be encountered as λ is decreased, although in our model only two of them can be the first bifurcation from homeotropy while only the other two can be the first bifurcation from isotropy. (It is likely that different models will allow other variations.) It then follows from the Equivariant Branching Lemma that each of the axial equilibrium types that we describe in Sec. III is an equilibrium solution to the nonlinear model equations.

III. SPATIALLY PERIODIC EQUILIBRIUM STATES

In this section we list the axial subgroups for each of the four representations of $\Gamma_{\mathcal{L}}$ on the square and hexagonal lattices, and then plot the planforms for the associated bifurcating branches from both the isotropic ($\eta<0$) and homeotropic ($\eta>0$) states. We emphasize that these results depend only on symmetry and can be obtained independently of any particular model. First, we describe the form of the eigenspaces for each of these four representations. Second, we discuss the group actions and the axial subgroups for each of these representations. Finally, we plot the associated direction fields.

A. Linear theory

Let L denote the linearization of the governing system of differential equations at Q_0 [for the free energy model with free energy $\mathcal{F}$ we have $\mathsf{L}=d^2F(Q_0)$]. Bifurcation occurs at parameter values where L has nonzero kernel. We prove that generically, at bifurcation to shortest dual wave vectors, $\ker \mathsf{L}$ has the form given in Theorem 3.1. Let

$$Q^{++}=\begin{bmatrix} a & 0 & 0 \\ 0 & b & 0 \\ 0 & 0 & -a-b \end{bmatrix}, \quad Q^{+-}=\begin{bmatrix} 0 & 0 & i \\ 0 & 0 & 0 \\ i & 0 & 0 \end{bmatrix},$$
$$Q^{-+}=\begin{bmatrix} 0 & 1 & 0 \\ 1 & 0 & 0 \\ 0 & 0 & 0 \end{bmatrix}, \quad Q^{--}=\begin{bmatrix} 0 & 0 & 0 \\ 0 & 0 & i \\ 0 & i & 0 \end{bmatrix}. \tag{1}$$

In the double superscript on Q, the first $\pm$ refers to scalar or pseudoscalar representation and the second $\pm$ refers to the action of τ. In Table I we also fix the generators of the lattice and its dual lattice.

TABLE I. Generators for the planar lattices and their dual lattices.

Lattice	ℓ_1	ℓ_2	$\mathbf{k}_1$	$\mathbf{k}_2$	$\mathbf{k}_3=-(\mathbf{k}_1+\mathbf{k}_2)$
Square	(1,0)	(0,1)	(1,0)	(0,1)	—
Hexagonal	$\left(1,\frac{1}{\sqrt{3}}\right)$	$\left(0,\frac{2}{\sqrt{3}}\right)$	(1,0)	$\frac{1}{2}(-1,\sqrt{3})$	$\frac{1}{2}(-1,-\sqrt{3})$

Theorem 3.1: *On the square lattice, let ξ be rotation counterclockwise by $\pi/2$. Then, in each irreducible representation,* $\ker \mathsf{L}$ *is four-dimensional and its elements have the form*

$$z_1 e^{2\pi i \mathbf{k}_1\cdot\mathbf{x}} Q^{\pm\pm} + z_2\, e^{2\pi i \mathbf{k}_2\cdot\mathbf{x}}\, \xi\cdot Q^{\pm\pm} + \text{c.c.} \tag{2}$$

for $z_1, z_2 \in \mathbf{C}$, where $Q^{\pm\pm}$ is the appropriate matrix specified in (1), $\xi\cdot Q$ denotes $\xi Q \xi^{-1}$, and c.c. *denotes complex conjugate.*

On the hexagonal lattice, let ξ be rotation counterclockwise by $\pi/3$. Then, in each irreducible representation, $\ker \mathsf{L}$ *is six-dimensional and its elements have the form*

$$z_1 e^{2\pi i \mathbf{k}_1\cdot\mathbf{x}} Q^{\pm\pm} + z_2\, e^{2\pi i \mathbf{k}_2\cdot\mathbf{x}}\, \xi^2\cdot Q^{\pm\pm} + z_3\, e^{2\pi i \mathbf{k}_3\cdot\mathbf{x}}\, \xi^4\cdot Q^{\pm\pm} + \text{c.c.} \tag{3}$$

for $z_1, z_2, z_3 \in \mathbf{C}$.

Proof: Let V and $V_{\mathbf{C}}$ denote the space of (respectively) real and complex 3×3 symmetric matrices with zero trace. Planar translation symmetry implies that eigenfunctions (nullvectors) of L are linear combinations of matrices that have the plane wave form

$$e^{2\pi i \mathbf{k}\cdot\mathbf{x}} Q + \text{c.c.}, \tag{4}$$

where $Q \in V_{\mathbf{C}}$ is a constant matrix and $\mathbf{k} \in \mathbf{R}^2$ is a wave vector. For fixed $\mathbf{k}$ let

$$W_{\mathbf{k}} = \{e^{2\pi i \mathbf{k}\cdot\mathbf{x}} Q + \text{c.c.} : Q \in V_{\mathbf{C}}\} \tag{5}$$

be the ten-dimensional L-invariant real linear subspace consisting of such functions.

Rotations and reflections $\gamma \in \mathbf{O}(2)\times\mathbf{Z}_2(\tau) \subset \mathbf{O}(3)$ act on $W_{\mathbf{k}}$ by

$$\gamma(e^{2\pi i \mathbf{k}\cdot\mathbf{x}} Q) = e^{2\pi i (\gamma\mathbf{k})\cdot\mathbf{x}}\, \gamma Q \gamma^{-1}. \tag{6}$$

When looking for nullvectors we can assume, after rotation, that $\mathbf{k} = k(1,0)$. We can also rescale length so that the dual wave vectors of shortest length have length 1; that is, we can assume that $k=1$.

Bosch Vivancos, Chossat, and Melbourne (1995) observed that reflection symmetries can further decompose $W_{\mathbf{k}}$ into two L-invariant subspaces. To see why, consider the reflection

$$\kappa(x,y,z) = (x,-y,z).$$

Note that the action (6) of κ on $W_{\mathbf{k}}$ (dropping the $+$c.c.) is

$$\kappa(e^{2\pi i \mathbf{k}\cdot\mathbf{x}} Q) = e^{2\pi i \kappa(\mathbf{k})\cdot\mathbf{x}}\, \kappa Q \kappa^{-1} = e^{2\pi i \mathbf{k}\cdot\mathbf{x}}\, \kappa Q \kappa^{-1}.$$

Since $\kappa^2 = 1$, the subspace $W_{\mathbf{k}}$ itself decomposes as

$$W_{\mathbf{k}} = W_{\mathbf{k}}^{+} \oplus W_{\mathbf{k}}^{-}, \tag{7}$$

where κ acts trivially on $W_{\mathbf{k}}^+$ and as minus the identity on $W_{\mathbf{k}}^-$, and each of $W_{\mathbf{k}}^+$ and $W_{\mathbf{k}}^-$ are L invariant. We call functions in $W_{\mathbf{k}}^+$ *even* and functions in $W_{\mathbf{k}}^-$ *odd*. Bifurcations based on even eigenfunctions are called *scalar* and bifurcations based on odd eigenfunctions are called *pseudoscalar*.

A further simplification in the form of Q can be made. Consider $\rho \in \mathbf{SO}(2) \subset \mathbf{O}(3)$ given by $(x,y,z) \mapsto (-x,-y,z)$. Since (dropping the $+$c.c.)

$$\rho(e^{2\pi i \mathbf{k}\cdot\mathbf{x}}Q) = e^{2\pi i \rho\mathbf{k}\cdot\mathbf{x}}\rho Q\rho^{-1} = e^{-2\pi i \mathbf{k}\cdot\mathbf{x}}\rho Q\rho^{-1} = e^{2\pi i \mathbf{k}\cdot\mathbf{x}}\overline{\rho Q\rho^{-1}}$$

the associated action of ρ on $V_{\mathbf{C}}$ is related to the conjugacy action by

$$\rho(Q) = \overline{\rho Q \rho^{-1}}. \tag{8}$$

Since L commutes with ρ and $\rho^2 = 1$, the subspaces of the kernel of L where $\rho(Q) = Q$ and $\rho(Q) = -Q$ are L-invariant. Therefore, we can assume that Q is in one of these two subspaces. Note moreover that translation by $\frac{1}{4}\mathbf{k}$ implies that if $e^{2\pi i \mathbf{k}\cdot\mathbf{x}}Q$ is an eigenfunction then $ie^{2\pi i \mathbf{k}\cdot\mathbf{x}}Q$ is a (symmetry related) eigenfunction. It follows from (8) that if ρ acts as minus the identity on Q, then ρ acts as the identity on iQ. Thus we can assume without loss of generality that up to translational symmetry Q is ρ-invariant, that is Q has the form

$$Q = \begin{bmatrix} a & g & ic \\ g & b & ih \\ ic & ih & -a-b \end{bmatrix},$$

where $a,b,c,g,h \in \mathbf{R}$. Therefore we have proved

Lemma 3.2: Up to symmetry eigenfunctions in $W_{\mathbf{k}}$ have the form

$$e^{2\pi i \mathbf{k}\cdot\mathbf{x}}Q + \text{c.c.}$$

where Q is nonzero, ρ-invariant, and either even or odd.

Lemma 3.2 implies that typically eigenfunctions in $W_{\mathbf{k}}$ lie in one of the two-dimensional subspaces $V_{\mathbf{k}}^+, V_{\mathbf{k}}^-$ of $W_{\mathbf{k}}^+, W_{\mathbf{k}}^-$ that have the form

$$V_{\mathbf{k}}^+ = \{ze^{2\pi i \mathbf{k}\cdot\mathbf{x}}Q^+ : z \in \mathbf{C}\},$$

$$V_{\mathbf{k}}^- = \{ze^{2\pi i \mathbf{k}\cdot\mathbf{x}}Q^- : z \in \mathbf{C}\},$$

where

$$Q^+ = \begin{bmatrix} a & 0 & ic \\ 0 & b & 0 \\ ic & 0 & -a-b \end{bmatrix} \quad \text{and} \quad Q^- = \begin{bmatrix} 0 & g & 0 \\ g & 0 & hi \\ 0 & hi & 0 \end{bmatrix} \tag{9}$$

with the specific values $a,b,c,g,h \in \mathbf{R}$ being chosen by L (cf. Golubitsky and Stewart, 2002, Sec. 5.7).

Moreover, since L commutes with τ we can further split

$$V_{\mathbf{k}}^+ = V_{\mathbf{k}}^{++} \oplus V_{\mathbf{k}}^{+-} \quad \text{and} \quad V_{\mathbf{k}}^- = V_{\mathbf{k}}^{-+} \oplus V_{\mathbf{k}}^{--}$$

into subspaces on which τ acts trivially and by minus the identity, and each of these subspaces is L-invariant. Since

TABLE II. (Left) $\mathbf{D}_4 \dotplus \mathbf{T}^2$ action on square lattice; (right) $\mathbf{D}_6 \dotplus \mathbf{T}^2$ action on hexagonal lattice. Here $[\theta_1,\theta_2]=\theta_1\ell_1+\theta_2\ell_2$ as in Table I. For scalar representation $\epsilon=+1$; for pseudoscalar representation $\epsilon=-1$.

$\mathbf{D}_4$	Action	$\mathbf{D}_6$	Action
$\mathbf{1}$	(z_1,z_2)	$\mathbf{1}$	(z_1,z_2,z_3)
ξ	(z_2,z_1)	ξ	(z_2,z_3,z_1)
ξ^2	(z_1,z_2)	ξ^2	(z_3,z_1,z_2)
ξ^3	(z_2,z_1)	ξ^3	(z_1,z_2,z_3)
κ	$\epsilon(z_1,z_2)$	ξ^4	(z_2,z_3,z_1)
$\kappa\xi$	$\epsilon(z_2,z_1)$	ξ^5	(z_3,z_1,z_2)
$\kappa\xi^2$	$\epsilon(z_1,z_2)$	κ	$\epsilon(z_1,z_3,z_2)$
$\kappa\xi^3$	$\epsilon(z_2,z_1)$	$\kappa\xi$	$\epsilon(z_2,z_1,z_3)$
		$\kappa\xi^2$	$\epsilon(z_3,z_2,z_1)$
		$\kappa\xi^3$	$\epsilon(z_1,z_3,z_2)$
		$\kappa\xi^4$	$\epsilon(z_2,z_1,z_3)$
		$\kappa\xi^5$	$\epsilon(z_3,z_2,z_1)$
$[\theta_1,\theta_2]$	$(e^{-2\pi i\theta_1}z_1,e^{-2\pi i\theta_2}z_2)$	$[\theta_1,\theta_2]$	$(e^{-2\pi i\theta_1}z_1,e^{-2\pi i\theta_2}z_2,e^{2\pi i(\theta_1+\theta_2)}z_3)$

$$\tau Q\tau=\begin{bmatrix} a & g & -ic \\ g & b & -ih \\ -ic & -ih & -a-b \end{bmatrix}$$

we see that $V_{\mathbf{k}}^{\pm\pm}=\{ze^{2\pi i\mathbf{k}\cdot\mathbf{x}}Q^{\pm\pm}:z\in\mathbf{C}\}$, where the matrices $Q^{\pm\pm}$ are as given in (1).

Finally, note that $\ker \mathsf{L}$ is invariant under the action of ξ. It follows that on the square lattice

$$\ker \mathsf{L}=V_{\mathbf{k}}^{\pm\pm}\oplus\xi(V_{\mathbf{k}}^{\pm\pm})$$

whereas on the hexagonal lattice

$$\ker \mathsf{L}=V_{\mathbf{k}}^{\pm\pm}\oplus\xi^2(V_{\mathbf{k}}^{\pm\pm})\oplus\xi^4(V_{\mathbf{k}}^{\pm\pm})$$

thus verifying (2), (3) and completing the proof of Theorem (3.1). □

B. Axial subgroups

The scalar and pseudoscalar actions of $\mathbf{E}(2)$ on the eigenfunctions on the square and hexagonal lattices are computed in Bressloff *et al.* (2001a). The results are given in Table II in terms of the coefficients z_j in (2) and (3).

The axial subgroups for each of the four irreducible representations of $\Gamma_{\mathcal{L}}$ are given in Table III, together with generators $(z_1,z_2)\in\mathbf{C}^2$ or $(z_1,z_2,z_3)\in\mathbf{C}^3$ (fixed vectors) of the corresponding one-dimensional fixed-point subspaces (axial eigenspaces) in $\ker \mathsf{L}$, and descriptions of the associated patterns (planforms).

The results in Table III summarize known results for scalar actions with and without the midplane reflection (Buzano and Golubitsky, 1983; Golubitsky *et al.*, 1984) and the less well known results for pseudoscalar actions (Bosch Vivancos *et al.*, 1995; Bressloff *et al.*, 2001a). See also Golubitsky and Stewart (2002). More precisely, on the hexagonal lattice, the scalar$^+$ action is identical to the action studied in Bénard convection (Busse, 1962; Buzano and Golubitsky, 1983) and the scalar$^-$ action is identical to the one studied in Bénard convection with the midplane reflection (Golubitsky *et al.*, 1984). The pseudoscalar$^+$ action is identical to that studied in Bosch Vivancos *et al.* (1995) and Bressloff *et al.* (2001a), whereas the pseudoscalar$^-$ action is again the same as the one in Bénard convection with the midplane reflection—but with different isotropy subgroups, as Figs. 5 and 6 show.

TABLE III. Summary of axial subgroups. On the hexagonal lattice in the scalar case with $\tau=+1$ the points (1,1,1) and $(-1,-1,-1)$ have the same isotropy subgroup $[\mathbf{D}_6(\kappa,\xi)\oplus\mathbf{Z}_2(\tau)]$—but are not conjugate by any element of $\Gamma_{\mathcal{L}}$. Therefore, the associated eigenfunctions generate different planforms.

Lattice	Planform	Axial isotropy subgroup	Fixed vector
		Scalar representation ($\epsilon=+1$); $\tau=+1$	
Square	Squares	$\mathbf{D}_4(\kappa,\xi)\oplus\mathbf{Z}_2(\tau)$	(1,1)
	Stripes	$\mathbf{Z}_2^2(\kappa\xi^2,\tau)\oplus\mathbf{O}(2)[\theta_2,\kappa]$	(1,0)
Hexagonal	Hexagons$^+$	$\mathbf{D}_6(\kappa,\xi)\oplus\mathbf{Z}_2(\tau)$	(1,1,1)
	Hexagons$^-$	$\mathbf{D}_6(\kappa,\xi)\oplus\mathbf{Z}_2(\tau)$	$(-1,-1,-1)$
	Stripes	$\mathbf{Z}_2^2(\kappa\xi^3,\tau)\oplus\mathbf{O}(2)[\theta_2,\kappa]$	(1,0,0)
		Pseudoscalar representation ($\epsilon=-1$); $\tau=+1$	
Square	Squares	$\mathbf{D}_4(\kappa[\frac{1}{2},\frac{1}{2}],\xi)\oplus\mathbf{Z}_2(\tau)$	(1,1)
	Stripes	$\mathbf{Z}_2^2(\kappa\xi^2[\frac{1}{2},0],\tau)\oplus\mathbf{O}(2)[\theta_2,\kappa[\frac{1}{2},0]]$	(1,0)
Hexagonal	Hexagons	$\mathbf{Z}_6(\xi)\oplus\mathbf{Z}_2(\tau)$	(1,1,1)
	Triangles	$\mathbf{D}_3(\kappa\xi,\xi^2)\oplus\mathbf{Z}_2(\tau)$	(i,i,i)
	Rectangles	$\mathbf{Z}_2^3(\kappa,\xi^3,\tau)$	$(0,1,-1)$
	Stripes	$\mathbf{Z}_2^2(\kappa\xi^3[\frac{1}{2},0],\tau)\oplus\mathbf{O}(2)[\theta_2,\kappa[\frac{1}{2},0]]$	(1,0,0)
		Scalar representation ($\epsilon=+1$); $\tau=-1$	
Square	Squares	$\mathbf{D}_4(\kappa,\xi)\oplus\mathbf{Z}_2(\tau[\frac{1}{2},\frac{1}{2}])$	(1,1)
	Stripes	$\mathbf{Z}_2^2(\kappa\xi^2,\tau[\frac{1}{2},0])\oplus\mathbf{O}(2)[\theta_2,\kappa]$	(1,0)
Hexagonal	Hexagons	$\mathbf{D}_6(\kappa,\xi)$	(1,1,1)
	Triangles	$\mathbf{D}_6(\kappa,\tau\xi)$	(i,i,i)
	Rectangles	$\mathbf{Z}_2^3(\tau\kappa,\xi^3,\tau[0,\frac{1}{2}])$	$(0,1,-1)$
	Stripes	$\mathbf{Z}_2^2(\kappa\xi^3,\tau[\frac{1}{2},0])\oplus\mathbf{O}(2)[\theta_2,\kappa]$	(1,0,0)
		Pseudoscalar representation ($\epsilon=-1$); $\tau=-1$	
Square	Squares	$\mathbf{D}_4(\tau\kappa,\xi)\oplus\mathbf{Z}_2(\tau[\frac{1}{2},\frac{1}{2}])$	(1,1)
	Stripes	$\mathbf{Z}_2^2(\kappa\xi^2[\frac{1}{2},0],\tau[\frac{1}{2},0])\oplus\mathbf{O}(2)[\theta_2,\kappa[\frac{1}{2},0]]$	(1,0)
Hexagonal	Hexagons	$\mathbf{D}_6(\tau\kappa,\xi)$	(1,1,1)
	Triangles	$\mathbf{D}_6(\tau\kappa,\tau\xi)$	(i,i,i)
	Rectangles	$\mathbf{Z}_2^3(\kappa,\xi^3,\tau[0,\frac{1}{2}])$	$(0,1,-1)$
	Stripes	$\mathbf{Z}_2^2(\kappa\xi^3[\frac{1}{2},0],\tau[\frac{1}{2},0])\oplus\mathbf{O}(2)[\theta_2,\kappa[\frac{1}{2},0]]$	(1,0,0)

C. The planforms

We now consider two-dimensional patterns by disregarding the z coordinate in $\mathbf{x}$ (but not in Q) and restricting attention to equilibrium states that are periodic with respect to a square or hexagonal lattice in the xy plane.

To visualize the patterns of bifurcating solutions we assume a layer of liquid crystal material in the xy plane that to first order has the form

$$Q(\mathbf{x})=Q_0+\varepsilon E(\mathbf{x}),$$

where E is an axial eigenfunction, ε is small, and Q_0 is either isotropic ($\eta=-1$) or homeotropic ($\eta=+1$). At each point (x,y) we represent the director field by a standard-length interval in the eigendirection corresponding to the largest eigenvalue of the symmetric 3×3 matrix $Q(\mathbf{x})$ at $\mathbf{x}=(x,y)$ and we plot only the projection of that interval in the xy plane. In this picture, a line element that degenerates to a point corresponds to a vertical eigendirection.

Suppose first that Q_0 is homeotropic. In this case the associated pattern is an array of points. Moreover, in our simulations no pattern will appear in bifurcations for which $Q(\mathbf{x})$ is fixed by the action of τ. For, if $E(\mathbf{x})\in V_{\mathbf{k}}^{++}$ or $V_{\mathbf{k}}^{-+}$ then

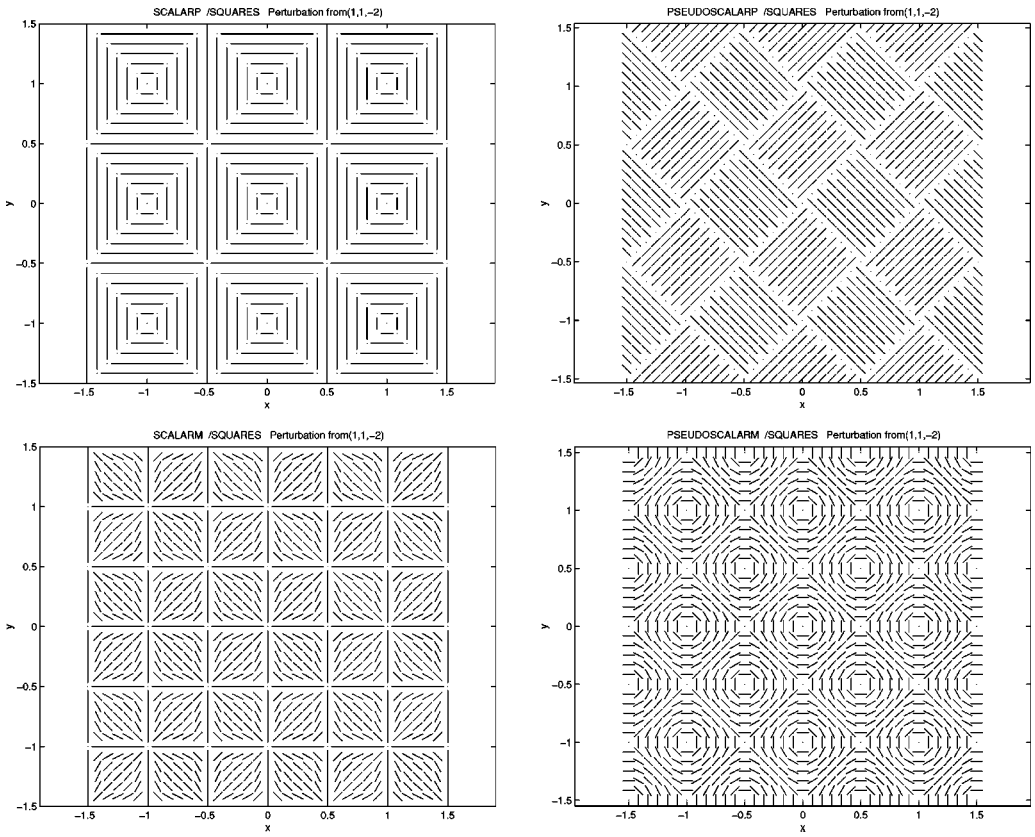

FIG. 3. Square lattice bifurcations from isotropic ($\eta<0$) liquid crystal to square patterns: (upper left) scalar $\tau=+1$; (upper right) pseudoscalar $\tau=+1$; (lower left) scalar $\tau=-1$; (lower right) pseudoscalar $\tau=-1$. Corresponding stripes patterns can be found in Figs. 1 and 7–10.

$$Q(\mathbf{x})=\begin{bmatrix} A & 0 \\ 0 & b \end{bmatrix},$$

where A is a 2×2 block and b is a scalar. Since b is close to 2 (the largest eigenvalue of Q_0) it is also the largest eigenvalue for $Q(\mathbf{x})$ for ε small. Hence, the leading eigendirection (corresponding to the largest eigenvalue) is always vertical and no patterns appear that are determined by changes in eigendirection. Nevertheless, since variation in the vertical eigenvalue of $Q(\mathbf{x})$ represents variation in the propensity of molecules to align vertically it is plausible that indistinct patterns could nevertheless be observed in practice.

Next suppose that Q_0 is planar isotropic. For small ε the director field is nearly horizontal (exactly horizontal if $\tau=+1$) and so our figures represent the pattern fairly accurately. When $\tau=-1$ there are small sinusoidal oscillations in the vertical component of the director field.

Bifurcations from isotropy exhibit lines or points of dislocation (where the director field is undefined) whereas bifurcations from homeotropy do not. In the latter case the director field is near vertical and there are small sinusoidal variations in the horizontal components. In this context the standard ''rolls'' terminology is misleading, as the director field is never horizontal: rather it oscillates about the vertical in a vertical plane and so generates ''stripes.''

In Figs. 3 and 4 we plot solutions corresponding to scalar and pseudoscalar square lattice patterns. In Figs. 5–10 we plot those for a hexagonal lattice. In the planforms obtained by bifurcation from homeotropy $\cdot$ indicates a vertical line element; whereas in the planforms obtained by bifurcation from isotropy $\cdot$ indicates points where $Q(\mathbf{x})$ has a double maximum eigenvalue,

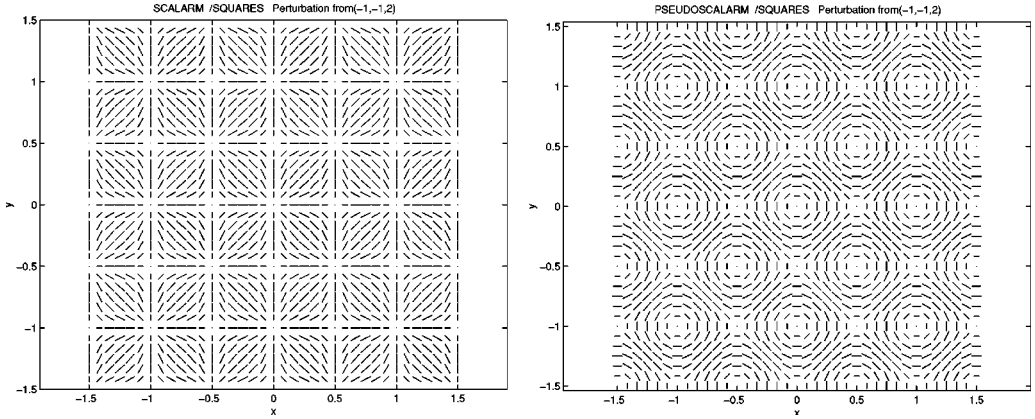

FIG. 4. Square lattice bifurcations from homeotropic ($\eta>0$) to squares with $\tau=-1$: (left) scalar; (right) pseudoscalar. Corresponding stripes patterns can be found in Figs. 5 and 6.

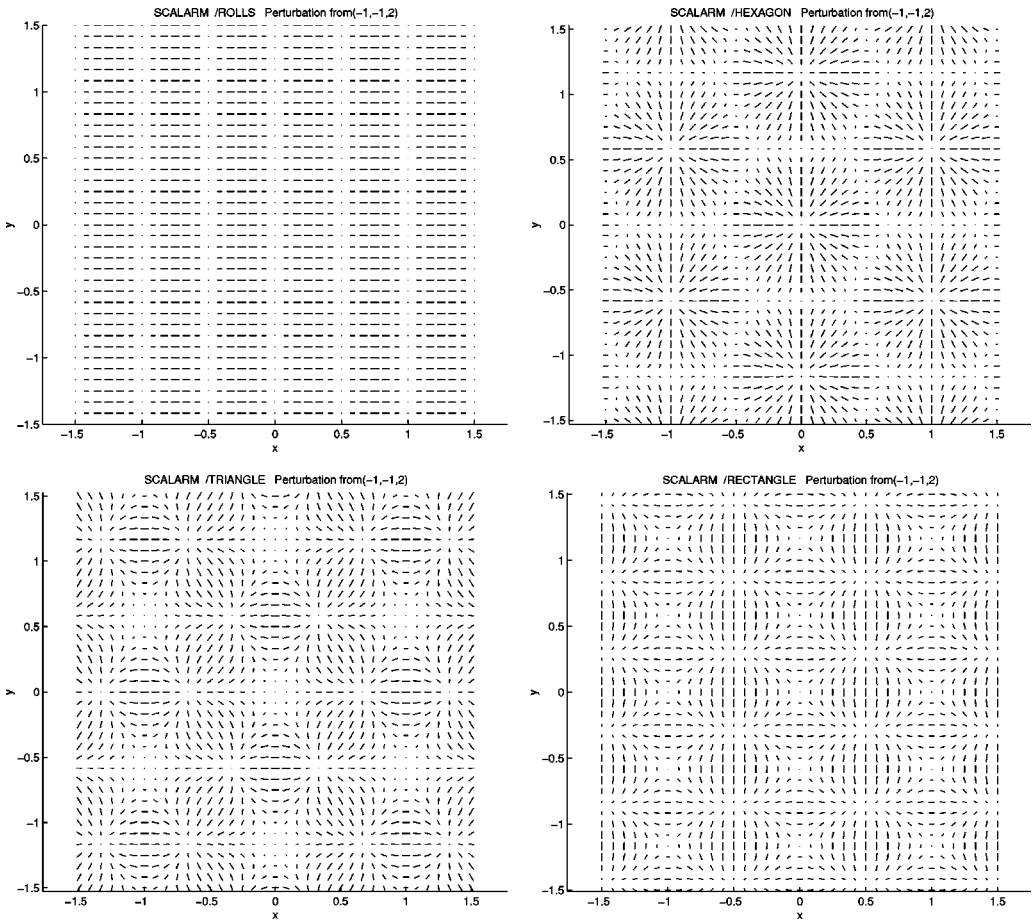

FIG. 5. Hexagonal lattice bifurcations from homeotropic ($\eta>0$) with scalar $\tau=-1$ representation: (upper left) stripes; (upper right) hexagons; (lower left) triangles; (lower right) rectangles.

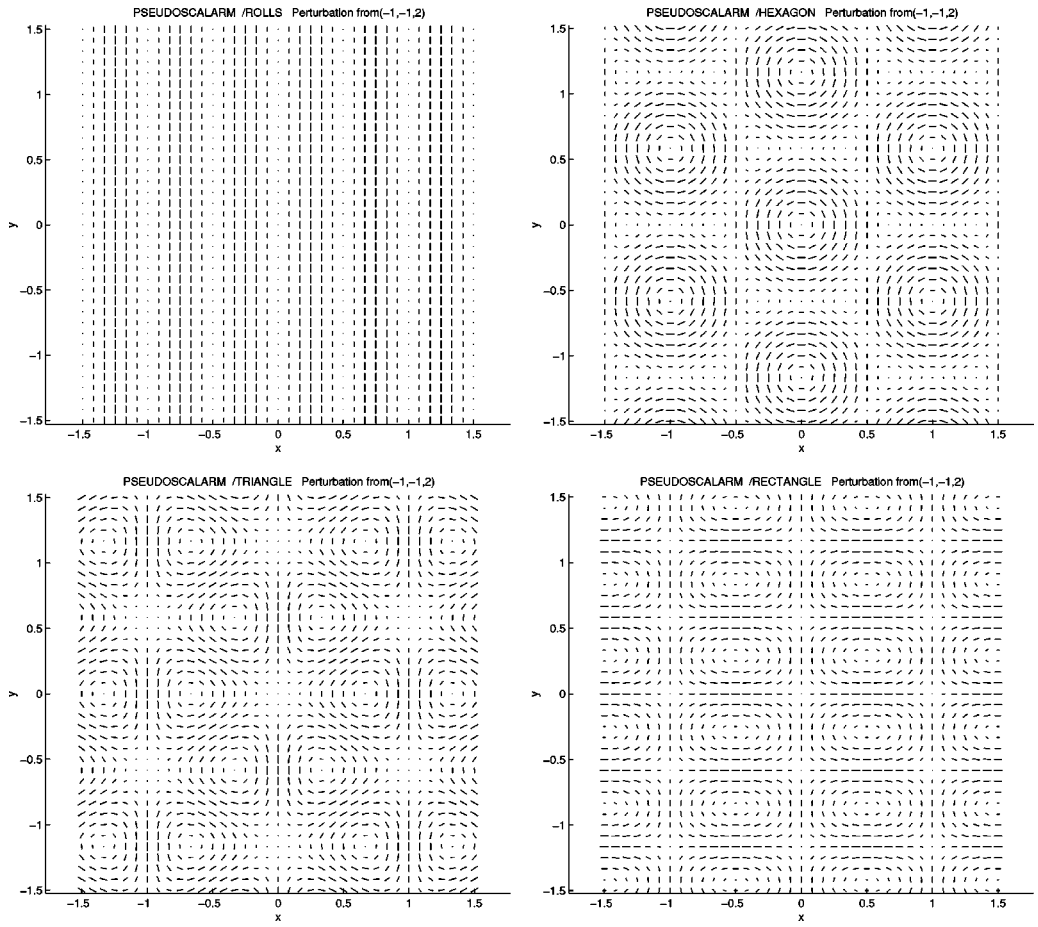

FIG. 6. Hexagonal lattice bifurcations from homeotropic ($\eta>0$) with pseudoscalar $\tau=-1$ representation: (upper left) stripes; (upper right) hexagons; (lower left) triangles; (lower right) rectangles.

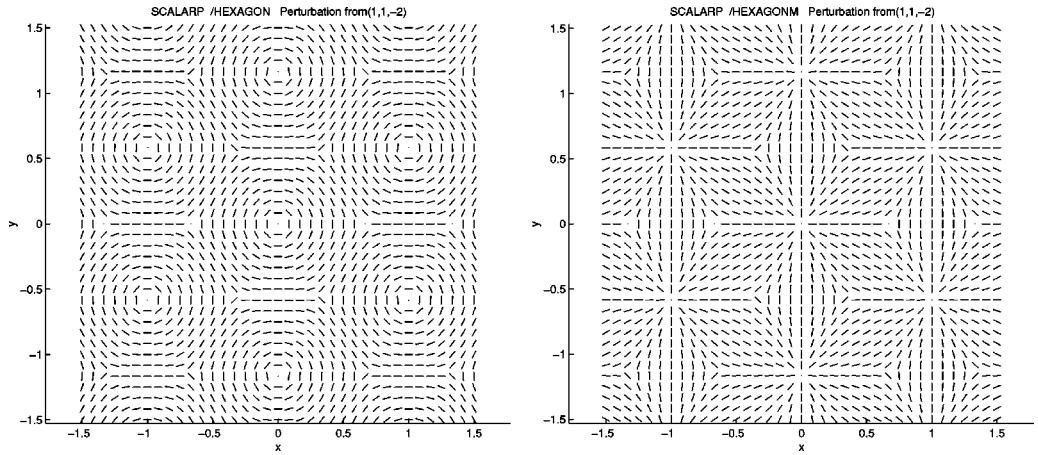

FIG. 7. Hexagonal lattice bifurcations from isotropic ($\eta<0$) with scalar $\tau=+1$ representation: stripes in Fig. 1; (left) hexagons^{+}; (right) hexagons^{-}.

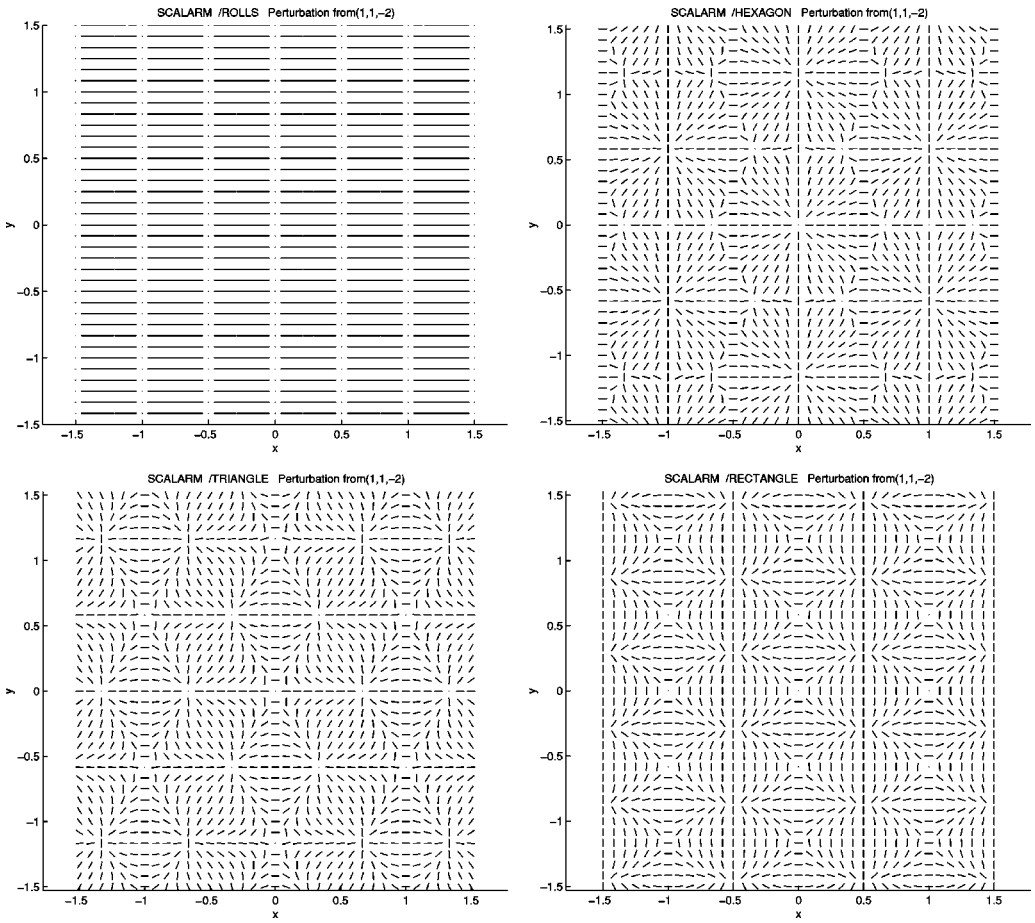

FIG. 8. Hexagonal lattice bifurcations from isotropic ($\eta<0$) with scalar $\tau=-1$ representation: (upper left) stripes; (upper right) hexagons; (lower left) triangles; (lower right) rectangles.

that is, a dislocation. Observe that across lines of dislocation the two competing directions are necessarily orthogonal in $\mathbf{R}^3$.

IV. FREE ENERGY MODELS

These results imply that for a planar liquid crystal there are four types of steady-state bifurcations, scalar, pseudoscalar, and $\tau=\pm 1$ of each type, that can occur from a spatially homogeneous equilibrium to spatially periodic equilibria. Whichever bifurcation occurs, then generically all of the planforms that we listed in the relevant section of Table III will be solutions. We have not discussed the difficult issue of stability of these solutions since these are model dependent results, whereas the classification of equilibria that we have given is independent of the model.

What remains is to complete a linear calculation to determine when a steady-state bifurcation occurs and whether it is scalar or pseudoscalar. The outline of such a calculation goes as follows. We first compute a *dispersion curve* for both scalar and pseudoscalar eigenfunctions. That is, for each wavelength $k=|\mathbf{k}|$ we determine the first value λ_k of the bifurcation parameter λ where L has a nonzero kernel. The curve (k,λ_k) is called the dispersion curve. We then find the minimum value $\lambda_*=\lambda_{k_*}$ on the dispersion curve; the corresponding wavelength k_* is the *critical* wavelength. We expect the first instability of the spatially homogeneous equilibrium to occur at the value λ_* of the bifurcation parameter. A bifurcating branch can consist of stable solutions only if the branch emanates from the first bifurcation (at λ_*).

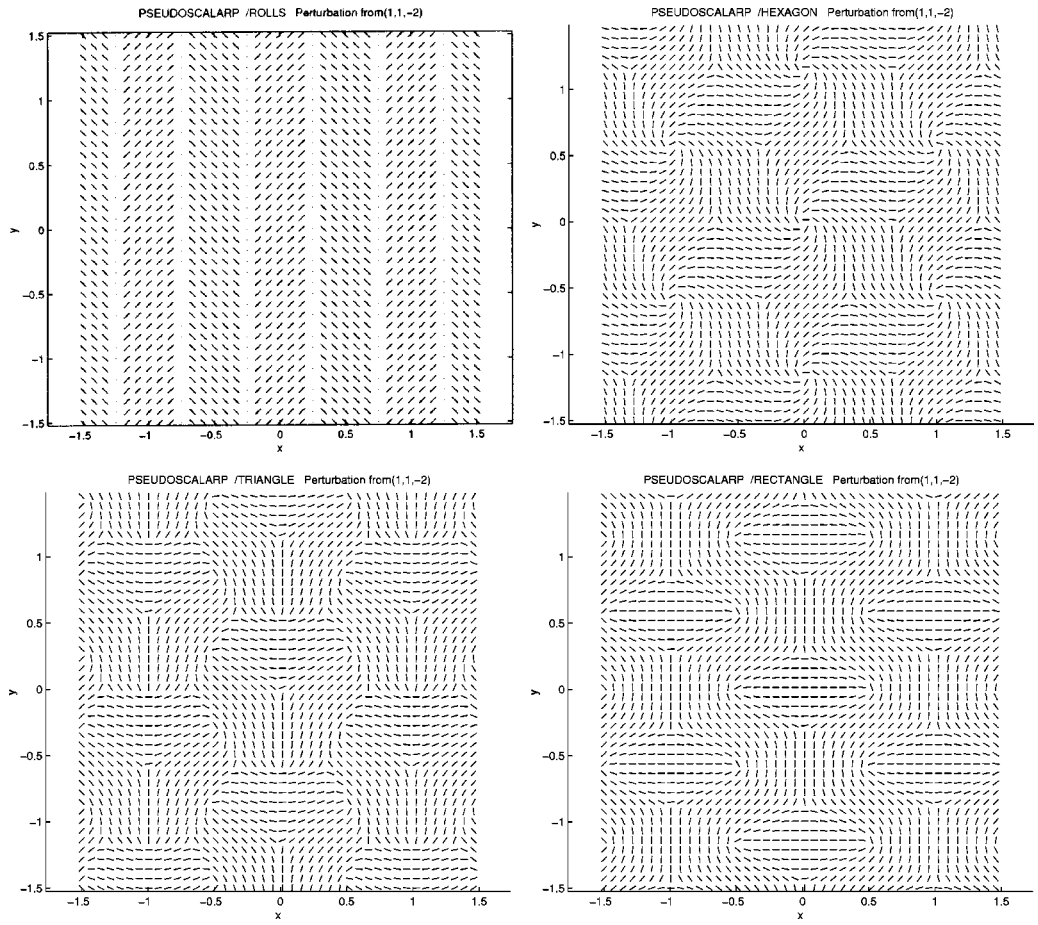

FIG. 9. Hexagonal lattice bifurcations from isotropic ($\eta<0$) with pseudoscalar $\tau=+1$ representation: (upper left) stripes; (upper right) hexagons; (lower left) triangles; (lower right) rectangles.

As an illustration we now carry out these calculations for a Landau–de Gennes type model with appropriate planar symmetry. Related calculations were carried out for bifurcation from the three-dimensional isotropic phase in Grebel *et al.* (1983). In this model we show that there are bifurcations corresponding to each of the four irreducible representations of $\Gamma_{\mathcal{L}}$, and which of them occurs first depends on the action of τ.

A. Dispersion curves for a two-dimensional Landau–de Gennes model

The free energy F is expressed as an integral per unit volume of a *free energy density* $\mathcal{F}$ which has two principal components $\mathcal{F}_0$ and $\mathcal{F}_d$ corresponding to *bulk terms* and *deformation terms*, respectively: we write F accordingly as $F=F_0+F_d$. For a system in three dimensions these typically [see, e.g., Grebel *et al.* (1983)] take the form

$$\mathcal{F}_0(Q)=\tfrac{1}{2}\lambda|Q|^2-\tfrac{1}{3}B\,\mathrm{tr}Q^3+\tfrac{1}{4}C|Q|^4,$$

$$\mathcal{F}_d(Q)=c_1|\nabla Q|^2+c_2|\nabla\cdot Q|^2+c_3|Q\cdot\nabla\wedge Q|,$$

respectively, where $|R|^2$ denotes the sum of the squares of the coefficients of the tensor R. The expression for $\mathcal{F}_0$ represents the simplest $\mathbf{SO}(3)$-invariant function on V exhibiting nontrivial interaction of local minima close to $Q=0$, while $\mathcal{F}_d$ consists of those $\mathbf{SO}(3)$-invariant terms of at most order 2 in spatial first derivatives (the chiral term $|Q\cdot\nabla\wedge Q|$ is not reflection-invariant).

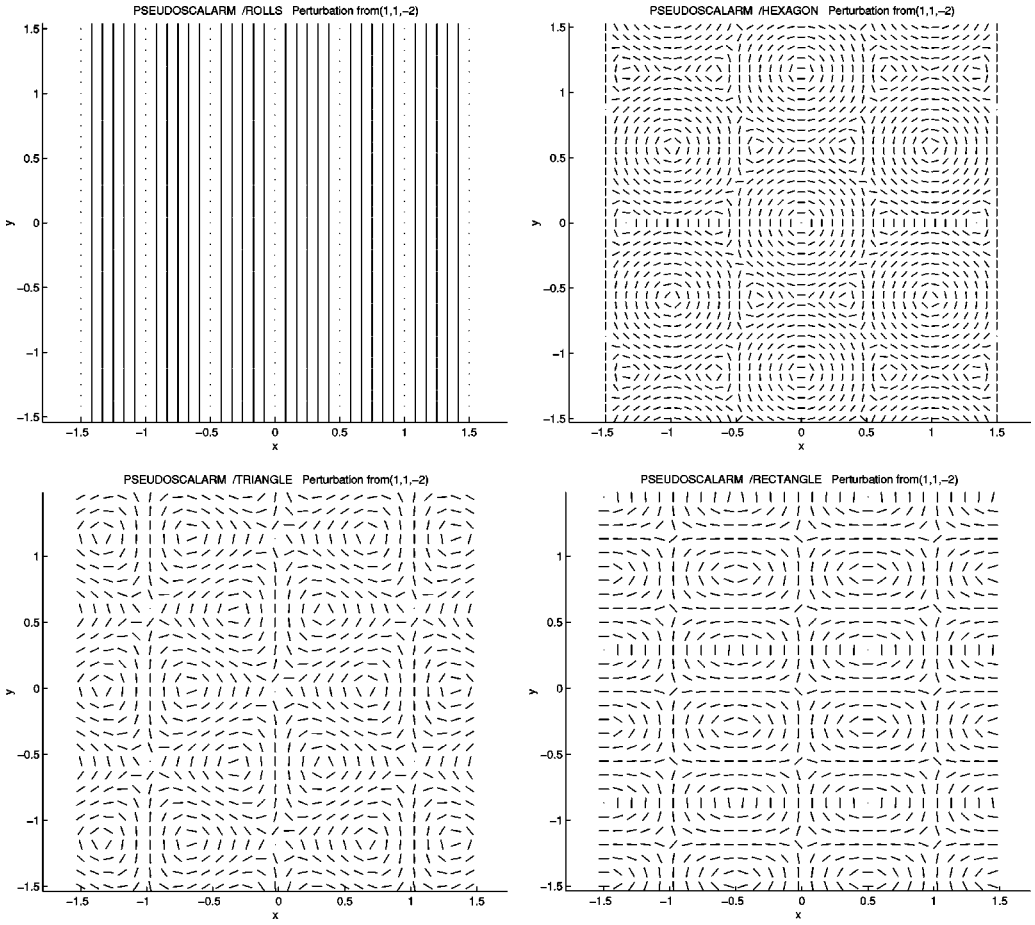

FIG. 10. Hexagonal lattice bifurcations from isotropic ($\eta<0$) with pseudoscalar $\tau=-1$ representation: (upper left) stripes; (upper right) hexagons; (lower left) triangles; (lower right) rectangles.

For a two-dimensional problem this choice of free energy function is not fully appropriate: the relevant symmetry group is now $\Gamma=\mathbf{E}(2)\times\mathbf{Z}_2(\tau)$. Consequently a wider range of terms can appear in $\mathcal{F}_0$, while the $|Q\cdot\nabla\wedge Q|$ term will no longer appear in $\mathcal{F}_d$.

We are interested in planforms that bifurcate from either the bulk homeotropic state or isotropic state, represented by Q_0 with $\eta>0$ or $\eta<0$, respectively. An example of a bulk term with $\mathbf{E}(2)\times\mathbf{Z}_2(\tau)$ invariance is $(Q_0\cdot Q)^2$, and a candidate for a deformation term to replace the chiral term is $|\Delta Q|^2$ representing longer range interactions of molecules. Accordingly we consider a free energy density $\mathcal{F}=\mathcal{F}_0+\mathcal{F}_d$ where now

$$\mathcal{F}_0(Q)=\tfrac{1}{2}\lambda|Q|^2-\tfrac{1}{3}B\mathrm{tr}Q^3+\tfrac{1}{4}C|Q|^4+\tfrac{1}{12}D(Q_0\cdot Q)^2,$$

$$\mathcal{F}_d(Q)=c_1|\nabla Q|^2+c_2|\nabla\cdot Q|^2+c_4|\Delta Q|^2.$$

Equilbrium states are critical points of F, and for $\mathcal{F}_0$ we have

$$d\mathcal{F}_0(Q)R=\lambda Q\cdot R-BQ^2\cdot R+C|Q|^2Q\cdot R+\tfrac{1}{6}D(Q_0\cdot Q)(Q_0\cdot R)$$

for arbitrary 3×3 real symmetric matrices Q,R; thus restricted to Q with trace zero we have $dF_0(Q)=0$ when

$$\lambda Q-B(Q^2-\tfrac{1}{3}|Q|^2I)+C|Q|^2Q+\tfrac{1}{6}D(Q_0\cdot Q)Q_0=0$$

TABLE IV. Computation of $d^2F(Q_0)R^2$.

R	$d^2F_0(Q_0)R^2$	$d^2F_d(Q_0)R^2$
$V_{\mathbf{k}}^{++}$	$\lambda(a^2+b^2-2ab)$ $-B(a^2+b^2+10ab)\eta$ $+6C(7(a^2+b^2)+10ab)\eta^2$	$2k^2(c_2a^2+$ $(a^2+b^2+(a+b)^2)(c_1+c_4k^2))$
$V_{\mathbf{k}}^{+-}$	$4(\lambda-B\eta+6C\eta^2)$ $=-4D\eta^2$ by (10)	$(4c_1+2c_2)k^2+4c_4k^4$
$V_{\mathbf{k}}^{-+}$	$4(\lambda+2B\eta+6C\eta^2)$	$(4c_1+2c_2)k^2+4c_4k^4$
$V_{\mathbf{k}}^{--}$	$4(\lambda-B\eta+6C\eta^2)$ $=-4D\eta^2$	$4c_1k^2+4c_4k^4$

and we easily verify the following:

$$dF_0(Q_0)=0\Leftrightarrow\lambda-B\eta+(6C+D)\eta^2=0. \tag{10}$$

Observe that $dF(Q)R=0$ automatically for any spatially periodic state R with zero mean, as the integral of an expression linear in R or its derivatives remains bounded as the volume tends to infinity. Therefore (10) is the condition for Q_0 to be an equilibrium state in our free energy model.

To study stability of the state Q_0 we evaluate the second derivative of the free energy at Q_0. For $R\in V$ we find

$$d^2F_0(Q_0)R^2=\lambda|R|^2-2BQ_0\cdot R^2+C(2(Q_0\cdot R)^2+|Q_0|^2|R|^2)+\tfrac{1}{6}D(Q_0\cdot R)^2$$

and (integrating over unit area)

$$d^2F_d(Q_0)R^2=c_1\int|\nabla R|^2+c_2\int|\nabla\cdot R|^2+c_4\int|\Delta R|^2$$

since Q_0 is spatially constant and terms linear in R integrate to zero.

We have already seen from Theorem 3.1 that the $\mathbf{E}(2)\times\mathbf{Z}_2(\tau)$ invariance of the free energy implies that generically the eigenfunctions of $d^2F(Q_0)$ on the space of $\mathcal{L}$-periodic matrix functions are linear combinations of functions belonging to one of the four subspaces $V_{\mathbf{k}}^{\pm\pm}$ and their rotations under $\pi/2$ (square lattice) or $\pm2\pi/3$ (hexagonal lattice). We next seek dispersion relations for each of the spaces $V_{\mathbf{k}}^{\pm\pm}$ in turn. When $R=e^{2\pi i\mathbf{k}\cdot\mathbf{x}}Q+$c.c. it is easy to check that

$$\frac{1}{4\pi^2}\int|\nabla R|^2=2k^2|Q|^2,\quad\frac{1}{4\pi^2}\int|\nabla\cdot R|^2=2|Q\mathbf{k}|^2,\quad\frac{1}{16\pi^4}\int|\Delta R|^2=2k^4|Q|^2,$$

where $k=|\mathbf{k}|$. Without loss of generality we can take $\mathbf{k}=(k,0,0)$ and then after rescaling k by a factor of 2π the evaluations of $d^2F_0(Q_0)R^2$ and $d^2F_d(Q_0)R^2$ are given in Table IV.

If we normalize by choosing D so that (10) is satisfied by $\eta=1$ (corresponding to homeotropy) then we find the conditions for a zero eigenvalue in each of the last three (one-dimensional) eigenspaces are, respectively,

$$\begin{aligned}\lambda-B+6C+(c_1+\tfrac{1}{2}c_2)k^2+c_4k^4=0,\\ \lambda+2B+6C+(c_1+\tfrac{1}{2}c_2)k^2+c_4k^4=0,\\ \lambda-B+6C+c_1k^2+c_4k^4=0\end{aligned} \tag{11}$$

with the analogous expressions for $\eta=-1$ (bifurcation from two-dimensional isotropy) obtained by merely reversing the sign of B in these equations.

Stationary values of λ as a function of k occur where

$$k^2 = -(c_1 + \tfrac{1}{2}c_2)/2c_4$$

for $V_{\mathbf{k}}^{+-}$ and $V_{\mathbf{k}}^{-+}$, or

$$k^2 = -c_1/2c_4$$

for $V_{\mathbf{k}}^{--}$, giving values

$$\lambda = \begin{cases} B - 6C + (c_1 + \frac{1}{2}c_2)^2/4c_4 & \text{for } V_{\mathbf{k}}^{+-} \\ -2B - 6C + (c_1 + \frac{1}{2}c_2)^2/4c_4 & \text{for } V_{\mathbf{k}}^{-+} \\ B - 6C + c_1^2/4c_4 & \text{for } V_{\mathbf{k}}^{--}. \end{cases} \tag{12}$$

Finally, if $R \in V_{\mathbf{k}}^{++}$ then the matrix for $d^2F_0(Q_0)R^2$ as a quadratic form in a,b is

$$\begin{bmatrix} \lambda - B + 42C & -\lambda - 5B + 30C \\ -\lambda - 5B + 30C & \lambda - B + 42C \end{bmatrix}$$

and for $d^2F_d(Q_0)R^2$ is

$$\begin{bmatrix} 4c_1k^2 + 2c_2k^2 + 4c_4k^4 & 2c_1k^2 + 2c_4k^4 \\ 2c_1k^2 + 2c_4k^4 & 4c_1k^2 + 4c_4k^4 \end{bmatrix}$$

and so $d^2F(Q_0)|V_{\mathbf{k}}^{++}$ has a nontrivial kernel when the determinant of the sum of these two matrices vanishes.

With $c_2 = 0$ (that is, in physical terms, with no energy cost to the molecules for ''splay'') the algebra simplifies to yield the dispersion relation

$$\lambda = -2B - 6C + \frac{c_1^2}{4c_4}. \tag{13}$$

From (11) and (13) we therefore see that with $c_2 = 0$ the values of λ for $V_{\mathbf{k}}^{\pm\pm}$ depend only on the second $\pm$, that is on whether bifurcating solutions have vertical reflection symmetry ($\tau = +1$) or not ($\tau = -1$) and are the same for the scalar and the pseudoscalar representations. Moreover, as λ decreases, the first bifurcation from the homeotropic state ($\eta > 0$) has $\tau = -1$ while the first bifurcation from the isotropic state ($\eta < 0$) has $\tau = +1$. These statements remain true for sufficiently small $|c_2|$.

B. Plausibility and applications

The models that we have described are of course mathematical idealizations of any real physical situation. In particular

(i) full two-dimensional Euclidean lattice symmetry (by its nature infinite) cannot exist in practice, and
(ii) the question of stability of the patterns has not been addressed.

Issue (i) arises in many areas of pattern formation, and it is a common observation that, despite the meaninglessness of full Euclidean lattice symmetry, the types of pattern that such symmetry predicts are indeed seen in physical situations over even fairly small regions. Moreover, attempts to force a planar solution into a sphere or other geometrical surface naturally lead to dislocations in the pattern. For liquid crystals these questions become particularly important in the context of membranes and other structures in biology [Brown and Wolken (1979)] where hexagonal patterns, for example, are not uncommon (although we make no claim to connect them directly

with the hexagonal planforms that we discuss). Our planar idealization may thus form a starting point for understanding two-dimensional pattern formation in more realistic contexts.

The very interesting question of stability of solutions (ii) is a mathematical issue that needs to be addressed on two levels. First, stability restricted to perturbations within the lattice should be considered. The general analysis has been worked out for the scalar representations (Buzano and Golubitsky, 1983; Golubitsky *et al.*, 1984) and discussed for the pseudoscalar $\tau=1$ (Bressloff *et al.*, 2001a), but has not been completed for the pseudoscalar $\tau=-1$ representation (though the analysis should be similar to the pseudoscalar $\tau=1$ case). A full treatment of this stability (based on symmetry and otherwise independent of the equations) will, even for our simplified model, require a long calculation and is beyond the scope of this work. We note that with the extra assumption of a free energy function it might be feasible to address even more general stability issues. However, we again believe that such efforts should be reserved for models more physically realistic than ours.

V. CONCLUSION

We have classified those square and hexagonally periodic patterns that are predicted to arise in the director field of a planar layer of a nematic liquid crystal when a homeotropic or planar isotropic state loses stability via the simplest spatially doubly periodic steady-state bifurcations. The techniques are those of group theory and representation theory, and are valid for any PDE model under various reasonable assumptions. If such patterns are observed experimentally, under conditions consistent with our assumptions, then our analysis provides the explanation: what remains is to evaluate relevant constants (on the basis of physical data) in order to determine *which* of the patterns is to occur. We have investigated some aspects of this for a Landau–de Gennes free energy model. Analogous methods to these have been used for some time in related fields such as Bénard convection, but for liquid crystal models the extra complexity of the matrix order parameter here gives a richer geometric structure.

ACKNOWLEDGMENTS

We are grateful to Tim Sluckin for instructive conversations on the mathematical physics of liquid crystals. We also wish to thank Greg Forest, Steve Morris, Axel Rossberg, and Ian Stewart for helpful conversations. The research of M.G. was supported in part by NSF Grant No. DMS-0071735 and ARP Grant No. 003652-0032-2001.

Bosch Vivancos, I., Chossat, P., and Melbourne, I., "New planforms in systems of partial differential equations with Euclidean symmetry," Arch. Ration. Mech. Anal. **131**, 199–224 (1995).

Bressloff, P., Cowan, J., Golubitsky, M., and Thomas, P., "Scalar and pseudoscalar bifurcations motivated by pattern formation on the visual cortex," Nonlinearity **14**, 739–775 (2001a).

Bressloff, P., Cowan, J., Golubitsky, M., Thomas, P., and Wiener, M., "Geometric visual hallucinations, Euclidean symmetry, and the functional architecture of striate cortex," Philos. Trans. R. Soc. London, Ser. B **356**, 299–330 (2001b).

Brown, G. and Wolken, J., *Liquid Crystals and Biological Structures* (Academic, New York, 1979).

Busse, F., "Das stabilitätsverhalten der zellarkonvektion bei endlicher amplitude," Ph.D. thesis, University of Munich, 1962.

Buzano, E. and Golubitsky, M., "Bifurcation involving the hexagonal lattice and the planar Bénard problem," Philos. Trans. R. Soc. London, Ser. A **308**, 617–667 (1983).

Chossat, P. and Lauterbach, R., *Methods in Equivariant Bifurcations and Dynamical Systems* (World Scientific, Singapore, 2000).

Cladis, P. and Palffy-Muhoray, P., editors, *Spatio-temporal Patterns in Nonequilibrium Complex Systems* (Addison–Wesley–Longman, Wellesley, MA, 1995).

Cross, M. and Hohenberg, P., "Pattern-formation outside of equilibrium," Rev. Mod. Phys. **65**, 851–1112 (1993).

de Gennes, P., *The Physics of Liquid Crystals* (Clarendon, Oxford, 1974).

Golubitsky, M. and Chillingworth, D., "Bifurcation and planar pattern formation for a liquid crystal," in *Conference on Bifurcations, Symmetry and Patterns, Porto 2000*, edited by J. Buescu, S. Castro, A. Dias, and I. Labouriau (Birkhäuser, Basel, 2003).

Golubitsky, M. and Stewart, I., *The Symmetry Perspective: From Equilibrium to Chaos in Phase Space and Physical Space*, Progress in Mathematics No. 200 (Birkhäuser, Basel, 2002).

Golubitsky, M., Stewart, I., and Schaeffer, D., *Singularites and Groups in Bifurcation Theory, II* (Springer, New York, 1988).

Golubitsky, M., Swift, J., and Knobloch, E., ''Symmetries and pattern selection in Rayleigh-Benard convection,'' Physica D **10**, 249–276 (1984).
Grebel, H., Hornreich, R., and Shtrikman, S., ''Landau theory of cholesteric blue phases,'' Phys. Rev. A **28**, 1114–1138 (1983).
Huh, J.-H., Hidaka, Y., Rossberg, A., and Kai, S., ''Pattern formation of chevrons in the conduction regime in homeotropically aligned liquid crystals,'' Phys. Rev. E **61**, 2769–2776 (2000).
Sluckin, T., ''The liquid crystal phases: physics and technology,'' Contemp. Phys. **41**, 37–56 (2000).